

Systematics of the $\sigma\tau_-$ strength in nuclei

G. Bertsch, D. Cha, and H. Toki

*National Superconducting Cyclotron Laboratory and Department of Physics,
Michigan State University, East Lansing, Michigan 48824*

(Received 10 February 1981)

The structure of the $\sigma\tau_-$ strength function is studied with a zero range interaction. The systematics of the giant Gamow-Teller state requires an interaction strength for $V_{\sigma\tau}$ of about 200–240 MeV fm³. While most of the strength goes to a state at high excitation, we find that $\sim 20-30\%$ of the strength remains at low excitation energy. The $L = 1$ states show considerable J splitting, with a major peak at ≈ 20 MeV excitation. This peak contains components of $J = 0, 1,$ and 2 . Comparison with the experimental $L = 1$ energy shows that the momentum dependence of the $\sigma\tau$ interaction is small.

[NUCLEAR STRUCTURE. Gamow-Teller states and $L = 1$ states in adjacent odd-odd mass nuclei of double closed shells. TDA and RPA calculation with zero range interaction.]

INTRODUCTION

The (p,n) reaction studies at intermediate energies have brought a tremendous advance in our empirical knowledge of the distribution of spin excitation strength in nuclei.¹⁻⁴ Qualitatively, the strength function has a peak in a state located at or above the position of the analog state. This state, the giant Gamow-Teller resonance, had been anticipated by theory for many years.⁵ In this article we wish to correlate the new data with a simple theoretical model. Our purpose is to extract from the data the properties of the residual interaction, rather than simply compare data with a particular interaction model, as has been done in other calculations of the Gamow-Teller strength.⁶ Our model is the Tamm-Dancoff approximation (TDA) based on the shell model wave functions from either a Woods-Saxon potential or a Skyrme Hartree-Fock calculation. We shall use a simple δ -function interaction and adjust the interaction strength so as to reproduce the main peak of the $\sigma\tau_-$ strength function. The model then gives predictions for the distribution of strength among 1p-1h configurations. As will be seen, roughly 20% of the strength appears in a state at much lower energy than the giant Gamow-Teller peak.

The same phenomenological interaction may also be applied to higher multipoles, for example, excitations induced by operators of the form $[Y_L(\theta)\sigma]_J\tau_-$. In principle, these higher multipoles will be sensitive to parts of the interaction that are

omitted in the δ -function treatment of the 1^+ excitations. Specifically, the momentum dependence of the interaction might affect the energies of the state with $L > 0$. However, we expect these effects to be small, and much can be learned with the momentum independent interaction. We shall discuss the effect of the momentum dependent interaction (finite range force) at the end. In examining the $L = 1$ strength function, we find a substantial splitting between different J states.

CALCULATIONAL DETAILS

Our model Hamiltonian consists of the single-particle Hamiltonian and the residual interaction. The single-particle Hamiltonian is spin dependent and possibly momentum dependent. As a model, we use a Woods-Saxon potential of standard parameters: $V_0 = 50$ MeV, $r_0 = 1.27$ fm, $A = 0.67$ fm. We shall also calculate the single-particle Hamiltonian within the Hartree-Fock theory with the Skyrme III interaction for comparison purposes.⁷ This model has an effective mass $m^*/m = 0.76$, close to what is expected from more fundamental Brueckner-Hartree-Fock theory. Besides the effective mass, another important question is the magnitude of the spin-orbit potential, since much of the excitation energy of the Gamow-Teller state arises from the spin-orbit splitting. The spin-orbit splitting of particles traveling at the Fermi momentum is about 6 MeV, but the direct observation of the splitting is difficult. The most direct evidence on the

strength of the spin-orbit interaction is probably obtained from elastic scattering. We therefore used a spin-orbit interaction from a global fit to low-energy elastic proton scattering data⁸ in the single-particle Hamiltonian based on the Woods-Saxon potential. The Skyrme III Hamiltonian includes a spin-orbit interaction which we used to make the spin-orbit

potential in this case.

As for the residual interaction, we take the spirit of the Landau-Migdal theory; i.e., the interaction matrix is the direct term of a δ -function interaction:

$$v_{\text{res}} = V_{\sigma\tau} \vec{\sigma}_1 \cdot \vec{\sigma}_2 \vec{\tau}_1 \cdot \vec{\tau}_2 \delta(\vec{r}_1 - \vec{r}_2)$$

The particle-hole matrix element is written as

$$\langle j_1 j_2^{-1} | v_{\text{res}} | j_3 j_4^{-1} \rangle_J = \frac{V_{\sigma\tau}}{4\pi} \int \phi_1 \phi_2 \phi_3 \phi_4 r^2 dr \sum_h^3 \langle j_1 j_2^{-1} | \sigma_h \rangle_J \langle j_3 j_4^{-1} | \sigma_{-h} \rangle_J, \quad (1)$$

where

$$\begin{aligned} \langle j_1 j_2^{-1} | \sigma_h \rangle_J &= \left[\frac{(j_1 + \frac{1}{2})(j_2 + \frac{1}{2})}{4\pi(2J+1)} \right]^{1/2} (-)^{J+1/2-j_1} (j_1 \frac{1}{2} j_2 - \frac{1}{2} | J0) [1 - (-)^{l_1+l_2-J}], \quad h=0 \\ \langle j_1 j_2^{-1} | \sigma_h \rangle_J &= \left[\frac{(j_1 + \frac{1}{2})(j_2 + \frac{1}{2})}{4\pi(2J+1)} \right]^{1/2} (-)^{J+1/2-j_1} (j_1 \frac{1}{2} j_2 - \frac{1}{2} | J0) \\ &\quad \times \frac{(-)^{j_1+j_2-J} (j_1 + \frac{1}{2}) + (j_2 + \frac{1}{2})}{[J(J+1)]^{1/2}} (-)^{l_1+l_2-L}, \quad h=+1 \\ \langle j_1 j_2^{-1} | \sigma_h \rangle_J &= \left[\frac{(j_1 + \frac{1}{2})(j_2 + \frac{1}{2})}{4\pi(2J+1)} \right]^{1/2} (-)^{J+1/2-j_1} (j_1 \frac{1}{2} j_2 - \frac{1}{2} | J0) \\ &\quad \times \frac{(-)^{j_1+j_2-J} (j_1 + \frac{1}{2}) + (j_2 + \frac{1}{2})}{[J(J+1)]^{1/2}}, \quad h=-1. \end{aligned}$$

With the above Hamiltonian we calculate the response to a $\sigma\tau$ field, using a Green's function technique in coordinate space developed by Bertsch and Tsai.⁹ We consider some nuclei with partially filled shells. These are treated in exactly the same way as closed shell nuclei, with fractional occupation numbers. Thus in ¹²⁴Sn in our models, the neutron Fermi level is in the $h_{11/2}$ shell, and this is given an occupancy factor of $\frac{1}{2}$ to make to total neutron number $N = 74$. It would be preferable to treat such nuclei in pairing theory, but we ignore such effects in this work.

The energy of excitation in the (p,n) reaction may be expressed in several ways: with respect to the ground state of the target nucleus, the ground state of the residual nucleus, or the analog state in the residual nucleus. From an experimental point of view the choice is strictly a matter of convenience, but the theory will involve different calculations in each case. The TDA theory requires as a starting point the single-particle energies in the residual nucleus. Given these energies, the interaction can then

be related quite directly to the excitation energy in the residual nucleus. We shall perform the calculation in this way. However, the single-particle energies are not really well known for heavy nuclei because there is an uncertainty in the momentum dependence of the single-particle Hamiltonian. Some of this ambiguity is removed if the energy of the spin excitations are compared to analog state energies.⁴ The analog state is made of $(j_p j_n^{-1})$ configurations, so the single-particle energies from these configurations just cancel out. The price one pays for using the analog state as an energy base is that the interaction energy of the analog state must then be computed. In attempting to do this, we were quite surprised to find substantial shell fluctuations in the analog energy in heavy nuclei that are probably not present in the data. We shall therefore calculate the excitation energy of the spin states with respect to the ground state of the residual nucleus.

The most important single-particle energies for the various nuclei we consider are shown in Table I. The second column gives the highest j occupied

TABLE I. Gamow-Teller energies: The energy of the main peak of the Gamow-Teller strength function is calculated in two models based on Woods-Saxon single particle energies and on Skyrme III single-particle energies. The residual interaction strength is $V_{\sigma\tau} = 220 \text{ MeV fm}^3$ for the Woods-Saxon model and 200 MeV fm^3 for the Skyrme model.

Nucleus	Highest j neutron orbit	$\epsilon(jj^{-1})$	Woods-Saxon		E	$\epsilon(jj^{-1})$	Skyrme III		Experimental E
			$\epsilon_{j_<} - \epsilon_{j_>}$	E			$\epsilon_{j_<} - \epsilon_{j_>}$	E	
⁴⁸ Ca	$f_{7/2}$	-0.2	6.0	10.3	-0.2	5.9	10.3	10.4 (Ref. 3)	
⁹⁰ Zr	$g_{9/2}$	-0.1	6.2	9.7	-0.1	5.8	9.4	8.2 (Ref. 1)	
⁹⁴ Zr								13.0 (Refs. 14,16)	
⁹⁶ Zr	$g_{9/2}$	5.1	6.1	15.1	5.6	5.5	15.3	13.7 (Refs. 14,16)	
¹¹² Sn	$g_{9/2}$	0.6	5.9	9.7	0.6	5.6	8.9	9.5 (Refs. 14,16)	
¹²⁴ Sn	$h_{11/2}$	2.9	6.6	14.1	4.3	6.6	13.7	13.9 (Refs. 14,16)	
¹⁶⁹ Tm	$h_{11/2}$	6.2	6.2	16.5	6.4	5.8	14.6	15.5 (Refs. 14,16)	
²⁰⁸ Pb	$i_{13/2}$	3.6	6.6	14.7	5.0	5.4	13.3	15.5 (Refs. 14,16)	

neutron orbit. The excitation energy of this configuration, $(j_p j_n^{-1})$, is shown in the column labeled $\epsilon(jj^{-1})$. For ⁴⁸Ca and ⁹⁰Zr this is the ground-state configuration, so the excitation energy is zero for the single-particle Hamiltonian. This has been corrected for the empirical interaction energy of the proton and neutron hole in the ground state. For the other nuclei, the $\epsilon(jj^{-1})$ energy is just the difference in single-particle energies of the jj^{-1} configuration and the ground-state configuration.

RESULTS

Experimentally, the main peak of the Gamow-Teller strength lies at an excitation energy of 9–15 MeV, and the available data can be reproduced to within about one MeV using the Woods-Saxon single-particle model and a residual interaction strength of

$$V_{\sigma\tau} = 220 \text{ MeV fm}^3 .$$

The comparison of theory and experiment is shown in Table I. The experimental energy is a mean energy including the $T_>$ strength, where it is known. Note that for the lighter nuclei, most of the excitation can be ascribed to the single-particle excitation energy of the $(j_< j_>^{-1})$ configuration. As $(N-Z)/A$ increases, the residual interaction energy increases, and with the nucleus ²⁰⁸Pb the interaction energy raises the state ~ 5 MeV higher than the $(j_< j_>^{-1})$ configuration. Clearly, the value we deduce for the residual interaction strength will depend on the assumed strength of the spin-orbit splitting. It is encouraging therefore that the Skyrme III Hamiltonian has nearly identical spin-orbit splittings for the lighter nuclei. In Pb, the Skyrme III spin-orbit splitting is about 1 MeV less

than the Becchetti-Greenlees, probably because the latter potential has too small a radius for heavy nuclei.

Examining Table I in more detail, it may be seen that the predicted energies for ⁹⁰Zr, ¹²⁴Sn, and ¹⁶⁹Tm are too high, and the remaining ones are low. No significance should be attached to the ¹⁶⁹Tm result because deformation effects are not included in the model. The ²⁰⁸Pb is nearly 1 MeV too low, and we shall see a possible reason for this when we discuss effects of the range of the residual interaction.

Although most of the strength is in the state at high excitation, there remains $\approx 20\%$ of the total strength at low excitation, which is also in a single state in the lighter nuclei. This double peak structure can be traced to the unperturbed configuration $(j_> j_>^{-1})$ and $(j_< j_>^{-1})$, which received roughly equal strength before the interaction is turned on. A simple estimate of the strength left in the lower state can be made by perturbation theory, starting from $L-S$ coupling rather than $j-j$ coupling. In the limit of strong residual interaction, the upper state has primarily $L=0$ character with roughly equal amplitudes of $j_>$ and $j_<$. The one-body spin-orbit field could then be considered by perturbation theory mixing upper and lower states with a matrix element of the order of $V \approx \frac{1}{2}(\epsilon_> - \epsilon_<) \approx 3 \text{ MeV}$. In this sense the splitting of the $L-S$ coupling state due to the residual interaction is $\approx 6 \text{ MeV}$ in the lighter nuclei. So the probability of the $L=0$ strength in the lower state would be estimated to be

$$P \approx \left[\frac{V}{\Delta E} \right]^2 \approx \left(\frac{3}{6} \right)^2 = \frac{1}{4} .$$

TABLE II. Gamow-Teller strength at low excitation. The fraction of the total strength below the major peak is shown.

Nucleus	Character	Low strength	
		Theory	Experiment
⁴⁸ Ca	single state	0.20	0.17 (Ref. 3)
⁹⁰ Zr	single state	0.20	0.25 (Ref. 1)
⁹⁶ Zr	several states	0.28	
¹¹² Sn	several states	0.28	
¹²⁴ Sn	several states	0.20	
¹⁶⁹ Tm	several states	0.27	
²⁰⁸ Pb	several states	0.28	

This probability is important for inferring the interaction. As we saw before, the calculation of the total excitation energy leaves some doubt as to the relative importance of the spin-orbit interaction and the residual interaction. These energies come in P in opposite ways however, and so, in principle, allow both to be determined. Our detailed calculation of P is shown in Table II compared with experiment. For the two cases that have been measured, there is good agreement between theory and experiment.

The excitation energies of the lower states may also be compared with experiment for the cases of ⁴⁸Ca and ⁹⁰Zr. These are shown in Table III. We see that these energies are too low. This is due to the inadequacy of the zero-range interaction for describing states which have substantial components of unnatural L , as will be seen later.

THE $L = 1$ STATES

Experimentally, an $L = 1$ peak is found in the (p, n) reaction at an excitation energy of ≈ 20 MeV. The available experimental data is collected in Table IV. It is reasonable to suppose that the strength is associated with spin flip, because the peak remains

TABLE III. Excitation energy of low-lying 1^+ state. Theory is with $V_{\sigma\tau} = 220 \text{ MeV fm}^3$, corrected for the empirical interaction energy of the ground state configuration.

Nucleus	$E(1^+)$	
	Theory	Experiment
⁴⁸ Ca	1.8	2.5 (Ref. 3)
⁹⁰ Zr	1.6	2.1 (Ref. 1)

prominent at 200 MeV bombarding energy, where $S = 0$ transfer is considerably suppressed in the (p, n) reaction. Coupling $S = 1$ to $L = 1$, the individual states will have total angular momentum 0, 1, and 2. The relative strength of the different J components is proportional to $(2J + 1)$ in the simple models, and detailed calculations will give results close to this limit.

The theoretical $L = 1$ strength function has a substantial splitting among different J values, with $J = 0$ highest in energy. This can be ascribed mainly to the one-body spin-orbit potential. Much of the $J = 0$ strength arises from states of the type

$$|(l' \frac{1}{2})_j (l \frac{1}{2})_j^{-1}\rangle_{J=0} \\ = |(l + 1, \frac{1}{2})_{l+1/2} (l \frac{1}{2})_{l+1/2}^{-1}\rangle_{J=0},$$

which has a large repulsive spin-orbit interaction. The $J = 2$ states, on the other hand, have quite a small expectation of the spin-orbit field. For the $J = 1$ and $J = 0$ states, a single eigenstate has nearly all of the strength. For the $J = 2$, however, the strength is spread over several states. These qualitative features were found in a calculation of ²⁰⁸Pb by Krmptović *et al.*¹⁰

Our calculation of the $(rY_1\sigma)_J$ strength in ⁹⁰Zr, shown in Fig. 1, also illustrates these points. The single-particle excitation energy in ⁹⁰Zr is about 9 MeV, except for spin-orbit splitting. The residual interaction shifts the strength upward by 5–10 MeV. In $L = 1$, there is significant strength for the τ_+ operator, and the resulting random-phase approximation (RPA) correlations lower the energy by about 1 MeV. We therefore use the RPA theory for calculations in this section. To facilitate com-

TABLE IV. $L = 1$ strength. The strength for the $(rY_1\sigma)_J$ operator is summed with a $(2J + 1)$ weighting. The position of the maximum of the theoretical strength is compared with the experimental $L = 1$ peak position. Energies are excitation in the residual nucleus.

Nucleus	E_{max}	E_{exp}
⁴⁸ Ca	22.0	
⁹⁰ Zr	20.0	17.3
⁹⁶ Zr	23.4	
¹¹² Sn	19.1	16.5
¹²⁴ Sn	23.1	19.4
¹⁶⁹ Tm	23.5	21.8
²⁰⁸ Pb	21.3	21.9

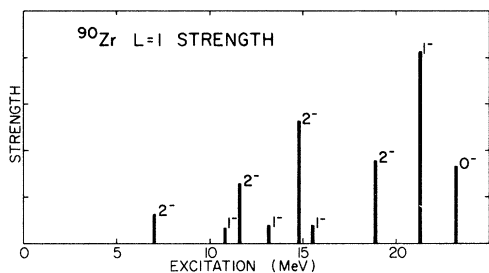


FIG. 1. The $L = 1$ strength in ^{90}Zr as a function of excitation energy. Numbers beside solid bars denote the J values.

parison with experiment, we have summed the strength functions for the different J 's in Fig. 2, and smoothed the sum with a Lorentzian function. The structure from the individual states disappears with a 4 MeV full width at half maximum (FWHM), which is what we used in Fig. 2. The different J states combine to give a broad peak at 20 MeV. There is a wide shoulder on the low energy side, composed primarily of $J = 2$. The median energy is about 18 MeV. If the smoothing function were made broader, so that the strength appeared as a single peak, the width would be ≈ 15 MeV.

Quite similar results are obtained with the Woods-Saxon and the Skyrme Hamiltonians. It might be expected that the strength would be higher

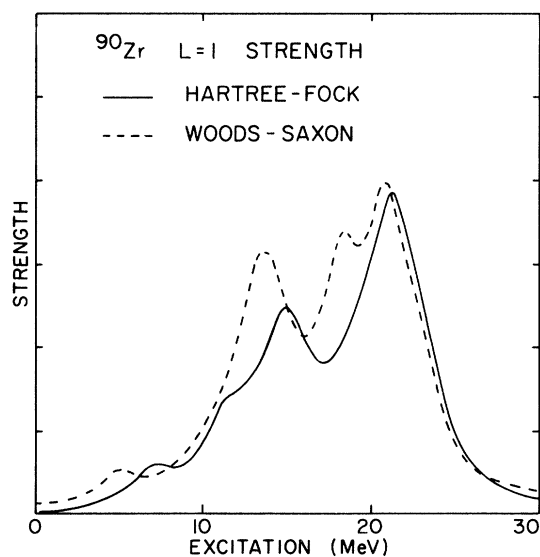


FIG. 2. The $L = 1$ strength in ^{90}Zr after smoothing out each state in Fig. 1 with a Lorentzian function of a 4 MeV FWHM width. The results with the Woods-Saxon and the Hartree-Fock wave functions are denoted by solid and dotted lines respectively.

in the Skyrme theory because of the larger single particle energy gaps. There is an effect of this sort, but it is small because the dominant orbits are in the surface, and is negated by a weaker spin-orbit field.

The experimentally observed $L = 1$ peak can be identified with the upper component of the theoretical strength of Fig. 2. The question then arises as to why the lower component has not been noticed in the experimental data. Perhaps its proximity to the Gamow-Teller peak has prevented an identification. In Table IV we quote the energy of the upper $L = 1$ peak for the different nuclei. The theoretical energy is determined graphically from the summed strength function, using the same smoothing as for ^{90}Zr .

We see that the excitation energy is nearly independent of A , unlike the Gamow-Teller energy. Heavier nuclei, with the larger mass asymmetry, have more interaction energy, but the single-particle excitation across major shells is less. These two tendencies cancel in the global trends.

Compared to experiment, the $L = 1$ energies are somewhat high. One possible reason is that the theoretical energy includes all isospins. This should agree with the experimental energy if the experimental fit included both the $T_>$ and $T_<$ strengths. Otherwise, if only $T_<$ strength is in the fit peak, the experimental number should be raised by about an MeV before comparing with theory. Another possible reason for the disagreement is the presence of $L = 1$ strength below the identified peak. If the spreading of the strength were greater, the theoretical peak would move to lower energy.

In view of these uncertainties, we can only draw tentative conclusions about the aspects of the residual interaction specifically tested by the $L = 1$ states. It appears that the predicted energy is too high, in which case an attractive momentum dependence is required in the $\sigma\tau$ interaction. From the qualitative formula of And \bar{o} ,¹¹ a shift of 2 MeV at 18 MeV requires that the Landau parameter G_1' be of the order

$$G_1' \approx 3\left[\left(\frac{18}{20}\right)^2 - 1\right] = -0.6 .$$

By contrast, the value deduced from the Reid potential is close to zero.¹²

It would be interesting to observe the predicted J splitting of the states. In principle, this could be done by observing the spin parameters of the reaction. To see how this works, we use a coordinate system with the z axis along the direction of momentum transfer. Then the orbital excitation has $M_L = 0$ in this coordinate system. If the spin

transfer is produced only by the operator σ_z , as would be the case for the non-spin-flip reaction shown in Fig. 3(a), the spin transfer is $M_s = 0$ and this reaction could only excite $J = 0$ and 2 states since the transferred angular momentum and the spin are $L = 1$ ($M_L = 0$) and $S = 1$ ($M_s = 0$) in this case, the total spin J is constructed by the Clebsch-Gordan coefficient $(1010|J0)$, which is finite for $J = 0$ and 2 but zero for $J = 1$. If, on the other hand, the reaction is induced by the σ_{\pm} spin operator, as the spin-flip process shown in Fig. 3(b), the spin transfer is $M_s = 1$ and the reaction would only excite $J = 1$ and 2 states. Thus the position of $J = 0$ could be distinguished from $J = 1$ by comparing these two spin experiments. While the measurement is probably hard for the (p, n) reactions, it is certainly feasible for inelastic proton scattering. The σ_{τ_z} strength function, which is tested by the (p, p') reaction, should behave similarly to the σ_{τ_-} strength function.

Finally, it is of interest to ask what relative excitation of the $S = 0, L = 1$ state is compared to the $S = 1$ states. A (p, n) experiment by Sterrenburg *et al.*,¹⁴ on ^{90}Zr at relatively low energy found the $L = 1$ peak significantly higher than in Table III. A possible explanation is that the lower energy experiment excited $S = 0$ strength, located at higher energy. The theoretical energy of the state can be estimated from our knowledge of the giant dipole state. In ^{90}Zr , the giant dipole energy of 16.8 MeV consists of about 10 MeV of single-particle energy and 7 MeV of interaction energy. There are more configurations contributing to the charge exchange dipole.

The interaction energy is roughly proportional to the strength of the $(rY_1\tau)$ operator. The strength of this operator is larger in the charge exchange mode because there is less Pauli blocking. Quantitatively,

$$\frac{\langle rY_1\tau_- \rangle_{90}^2}{\langle rY_1\tau_z \rangle_{90}^2} \approx 1.45 .$$

The interaction energy is then $7 \times 1.45 \approx 10$

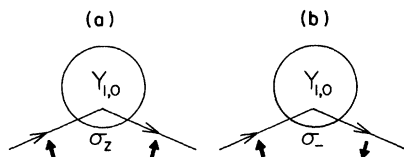


FIG. 3. Spin parameters of the $L = 1$ excitation. The thin line denotes the incoming and outgoing nucleon, with the thick arrows representing their spin directions.

MeV, and the excitation energy should be near 20 MeV. This accords with the findings of Ref. 14.

SIGNIFICANCE of $V_{\sigma\tau}$

The true interaction is quite complex, with the noncentral components and important finite range effects. The question arises as to how to make contact between the model discussed here and more elaborate descriptions of the interaction. Confining our attention to local interactions, some insight may be gained by examining the direct and exchange matrix elements separately.

The direct term in the residual interaction is simply a double convolution of the transition density with the interactions. The spatial variation of the transition density should be small on the scale of the interaction range for the δ interaction to accurately represent a finite range force of the same volume integral. The Gamow-Teller transition density has no spatial variation in tangential directions. However, the radial variation is significant when only a single l orbit is involved in the transition, as happens in the lighter nuclei considered. We shall estimate the effect of the finite range force on the volume integral by assuming that the radial dependence of the transition density is represented by a Gaussian,

$$\delta\rho(r) \sim e^{-\alpha(r-r_0)^2}, \quad \alpha \sim 0.7 \text{ fm}^{-2} . \quad (2)$$

The finite range integral of a Yukawa function is then reduced by a factor

$$R = \frac{\int d^3r d^3r' \delta\rho(r) \delta\rho(r') [\mu^2 e^{-\mu(r-r')} / 4\pi(r-r')] }{\int d^3r d^3r' \delta\rho(r) \delta\rho(r') \delta^3(r-r')} \\ \approx \left[\frac{\pi\mu^2}{2\alpha} \right]^{1/2} e^{\mu^2/2\alpha} \left\{ 1 - \text{erf} \left[\left[\frac{\mu^2}{2\alpha} \right]^{1/2} \right] \right\} . \quad (3)$$

In the last step the integral was evaluated replacing the spherical geometry by an infinite plane geometry. For the one-pion exchange potential, $\mu = 0.7 \text{ fm}^{-1}$, the reduction factor is 0.6. We have verified this reduction factor with more accurate calculations.

The exchange term is normally evaluated in a zero-range approximation. Namely, assume that the structure of the transition amplitude has equal contributions from all particle orbits on the Fermi surface. Then the transition density matrix may be approximated by the local Fermi gas approximation,

$$\delta\rho(r, r') \approx \delta\rho \left[\frac{r+r'}{2} \right] \int \frac{d\hat{k}}{4\pi} e^{ik_F \hat{k} \cdot (\vec{r} - \vec{r}')} . \quad (4)$$

The exchange matrix element of a Yukawa interaction of unit strength is then evaluated as

$$\begin{aligned} & \int [\delta\rho(r, r')]^2 \frac{\mu^2 e^{-\mu(r-r')}}{4\pi(r-r')} d^3r d^3r' \\ &= \int d^3R [\delta\rho(R)]^2 \int \frac{d\hat{k}}{4\pi} \frac{d\hat{k}'}{4\pi} \frac{\mu^2}{\mu^2 + |k_F \hat{k} - k_F \hat{k}'|^2} \\ &= \int d^3R [\delta\rho(R)]^2 \left[\frac{\mu^2}{4k_F^2} \ln \left(1 + \frac{4k_F^2}{\mu^2} \right) \right] . \end{aligned} \quad (5)$$

Substituting the pionic μ and $k_F = 1.35 \text{ fm}^{-1}$, the factor in brackets is $\frac{1}{3}$. This may be compared with a more careful evaluation of the exchange matrix element for the Gamow-Teller state in ^{48}Ca , which yields a reduction of $\frac{1}{4}$.

The approximation (4), upon which this argument is based, fails when the excitation is dominated by a single Slater determinant. Then the integrand in the exchange integral is non-negative, and the long-range components of the interaction are not suppressed. This happens in the 0^- states of light nuclei,¹⁵ which are nearly pure configurations. Also, very high spin states, such as $(j_{15/2} i_{13/2}^{-1})_{14^-}$ have this character. It is then necessary to treat the finite range of the force explicitly to describe all the properties of the states.¹⁵ The finite range enters crucially in another situation, when the state is predominantly unnatural multipolarity, $(-)^L \neq \Pi$. Then a zero-range interaction vanishes identically, but not the exchange of a finite range interaction. This is the situation with the lower 1^+ state. It is predominantly $L = 2, S = 0$, and the exchange interaction in this channel makes up the discrepancy in energy noted in Table III.

We are now in a position to relate $v_{\sigma\tau}$ to the conventional model of the interaction with explicit one-pion exchange,

$$V(q) = \vec{\tau} \cdot \vec{\tau}' \frac{f^2}{\mu^2} \left[g' \vec{\sigma} \cdot \vec{\sigma}' - \frac{\vec{q} \cdot \vec{\sigma} \vec{q}' \cdot \vec{\sigma}'}{q^2 + \mu^2} \right] , \quad (6)$$

where $f^2/\mu^2 \approx 390 \text{ MeV fm}^3$. In coordinate space this becomes

$$\begin{aligned} V(r) = \vec{\sigma} \cdot \vec{\sigma}' \vec{\tau} \cdot \vec{\tau}' \frac{f^2}{\mu^2} & \left[\left(g' - \frac{1}{3} \right) \delta^3(r - r') \right. \\ & \left. + \frac{1}{3} \frac{\mu^2}{4\pi} \frac{e^{-\mu r}}{r} \right] \\ & + \text{tensor} . \end{aligned} \quad (7)$$

Forgetting the tensor part, we obtain

$$\frac{\mu^2}{f^2} V_{\sigma\tau} \approx \left(g' - \frac{1}{3} + \frac{1}{3} R \right) \approx (g' - 0.12) \quad (8)$$

and we deduce

$$g' \approx (\mu^2/f^2) V_{\sigma\tau} + 0.12 \approx 0.56 + 0.12 = 0.68.$$

If the model includes the exchange of the one-pion exchange potential (OPEP) explicitly, then the interaction in the $\sigma\tau$ channel is

$$\begin{aligned} & \left(g' - \frac{1}{3} \right) \delta_D^3(r - r') \\ & + \frac{1}{12} \delta_E^3(r - r') + \frac{1}{3} \frac{\mu^2}{4\pi} \frac{e^{-\mu r}}{r} \Big|_D \\ & - \frac{1}{12} \frac{\mu^2}{4\pi} \frac{e^{-\mu r}}{r} \Big|_E , \end{aligned} \quad (9)$$

$$\begin{aligned} V_{\sigma\tau} \frac{\mu^2}{f^2} & \approx \left[g' - \frac{1}{3} (1 - R_D) \right. \\ & \left. + \frac{1}{12} (1 - R_E) \right] \approx g' - 0.07 . \end{aligned}$$

Thus the volume integral we deduce of 220 MeV fm^3 is consistent with a g' of the order of 0.6.

Concerning the tensor force, the contribution is expected to be small as compared to the central piece due to the fact that the main components of the particle-hole states with high j are $L = 0$. Furthermore, the actual calculation of the matrix elements in ^{48}Ca shows a large cancellation between the direct and exchange terms of the tensor force.

CONCLUSION

Stimulated by the recent experimental developments on the (p, n) reaction at intermediate energies on various nuclei, we have performed a systematic study of the giant Gamow-Teller states and the $L = 1$ states (most probably $S = 1$) in the whole

range of medium and heavy nuclei ($A \geq 48$). A simple theoretical model with a zero range interaction is used, which gives rise to a fairly nice description of these states. We found that the giant Gamow-Teller states are reproduced to within about 1 MeV using a constant spin-isospin strength; $V_{\sigma\tau} = 220 \text{ MeV fm}^3$. This value corresponds to the Landau parameter of $g' = 0.56$ when the OPEP is neglected. If the OPEP is considered, the estimated g' is of the order of 0.6, which is consistent with the general belief for this parameter.^{17,18} The resulting $M1$ strength is concentrated to the giant Gamow-Teller state, but about 20–30% of the strength is left at low excitation energy. This result agrees with the existing experimental results for ^{48}Ca and ^{90}Zr .

The $L = 1$ strength also has been considered within this simple model. The $L = 1$ strength (with $S = 1$) turns out to have a substantial splitting among different J values. Among the possible spins, $J = 0, 1$, or 2 , the $J = 0$ state stays at the

highest excitation due to the spin-orbit splitting. An experimental method to disentangle the J values is proposed. The theoretical strength is compared with the experimentally observed $L = 1$ peak. While the tendency that the $L = 1$ state remains at a constant value, about 20 MeV, with the mass number is reproduced, the excitation energy is calculated to be too high if one takes $V_{\sigma\tau} = 220 \text{ MeV}$, deduced from the $M1$ state. This must be related to the use of the zero-range interaction and it is interesting to study the finite range effect for these finite L states.

ACKNOWLEDGMENTS

The authors acknowledge valuable discussions with A. Galonsky, S. Austin, and B. H. Wildenthal. This work is supported by the National Science Foundation under Grant No. PHY 79-22054.

-
- ¹D. E. Bainum, J. Rapaport, C. D. Goodman, D. J. Horen, C. C. Foster, M. B. Greenfield, and C. A. Goulding, *Phys. Rev. Lett.* **44**, 1751 (1980).
- ²C. D. Goodman, C. A. Goulding, M. B. Greenfield, J. Rapaport, D. E. Bainum, C. C. Foster, W. G. Love, and F. Petrovich, *Phys. Rev. Lett.* **44**, 1975 (1980).
- ³B. D. Anderson, J. N. Knudsen, P. C. Tardy, J. W. Watson, R. Madey, and C. C. Foster, *Phys. Rev. Lett.* **45**, 699 (1980).
- ⁴D. J. Horen, C. D. Goodman, C. A. Goulding, M. B. Greenfield, J. Rapaport, D. E. Bainum, E. Sugarbaker, T. G. Masterson, F. Petrovich, and W. G. Love, *Phys. Rev. Lett.* **95B**, 27 (1980).
- ⁵K. Ikeda, S. Fujii, and J. I. Fujita, *Phys. Lett.* **3**, 271, (1963); see also, H. Ejiri and J. I. Fujita, *Phys. Rep.* **38C**, 85 (1978).
- ⁶C. Gaarde *et al.*, *Nucl. Phys.* **A334**, 248 (1980); S. Krewald, F. Osterfeld, J. Speth, and G. E. Brown, *Phys. Rev. Lett.* **46**, 103 (1981).
- ⁷M. Beiner, H. Flocard, N. Van Giai, and P. Quentin, *Nucl. Phys.* **A238**, 29 (1975).
- ⁸F. Becchetti and G. Greenless, *Phys. Rev.* **182**, 1190 (1969).
- ⁹G. Bertsch and S. F. Tsai, *Phys. Rep.* **18C**, 126 (1975).
- ¹⁰F. Krmpotić, K. Ebert, and W. Wild, *Nucl. Phys.* **A342**, 497 (1980); F. Krmpotić, *ibid.* **A351**, 365 (1981).
- ¹¹K. Andō, see Ref. 13, p. 192.
- ¹²S. O. Bäckman *et al.*, *Nucl. Phys.* **A321**, 10 (1979).
- ¹³T. Suzuki and M. Oka, in *Proceedings of the International Conference on Nuclear Physics, Berkeley, 1980*, p. 112.
- ¹⁴W. A. Sterrenburg, S. M. Austin, R. P. Devito, and A. Galonsky, *Phys. Rev. Lett.* **45**, 1839 (1980).
- ¹⁵J. Meyer-ter-Vehn, in *Phys. Rep.* (to be published).
- ¹⁶A. Galonsky and T. Nees, private communication; D. J. Horen, C. D. Goodman, D. E. Bainum, C. C. Foster, C. Gaarde, C. A. Goulding, M. B. Greenfield, and J. Rapaport, *Phys. Lett.* **99B**, 383 (1981).
- ¹⁷H. Toki and W. Weise, *Phys. Lett.* **92B**, 265 (1980); **97B**, 12 (1980).
- ¹⁸J. Speth, V. Klemt, J. Wambach, and G. E. Brown, *Nucl. Phys.* **A343**, 382 (1980).